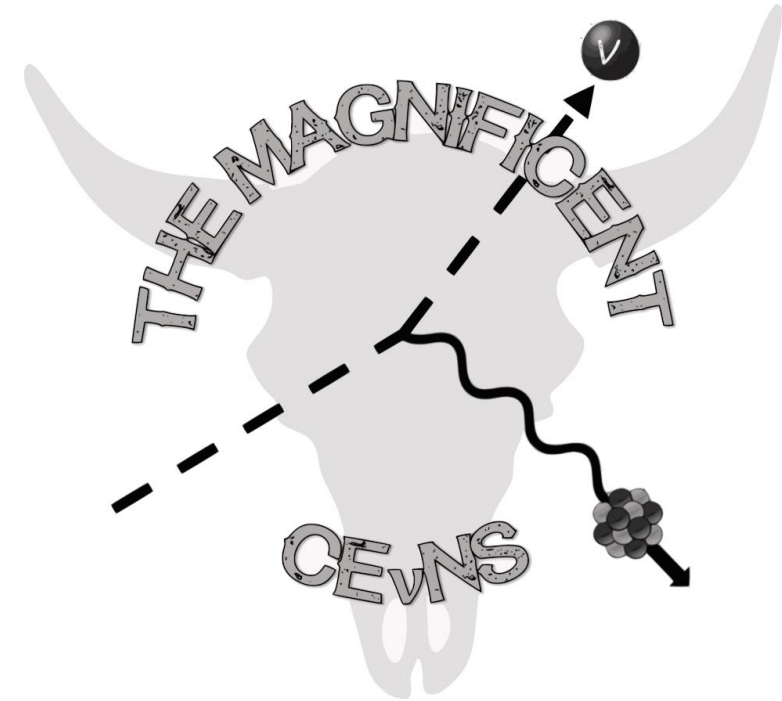


Magnificent CEvNS, November 16-20 2020, Cyberspace



COHERENT at SNS and Csl[Na] effort update

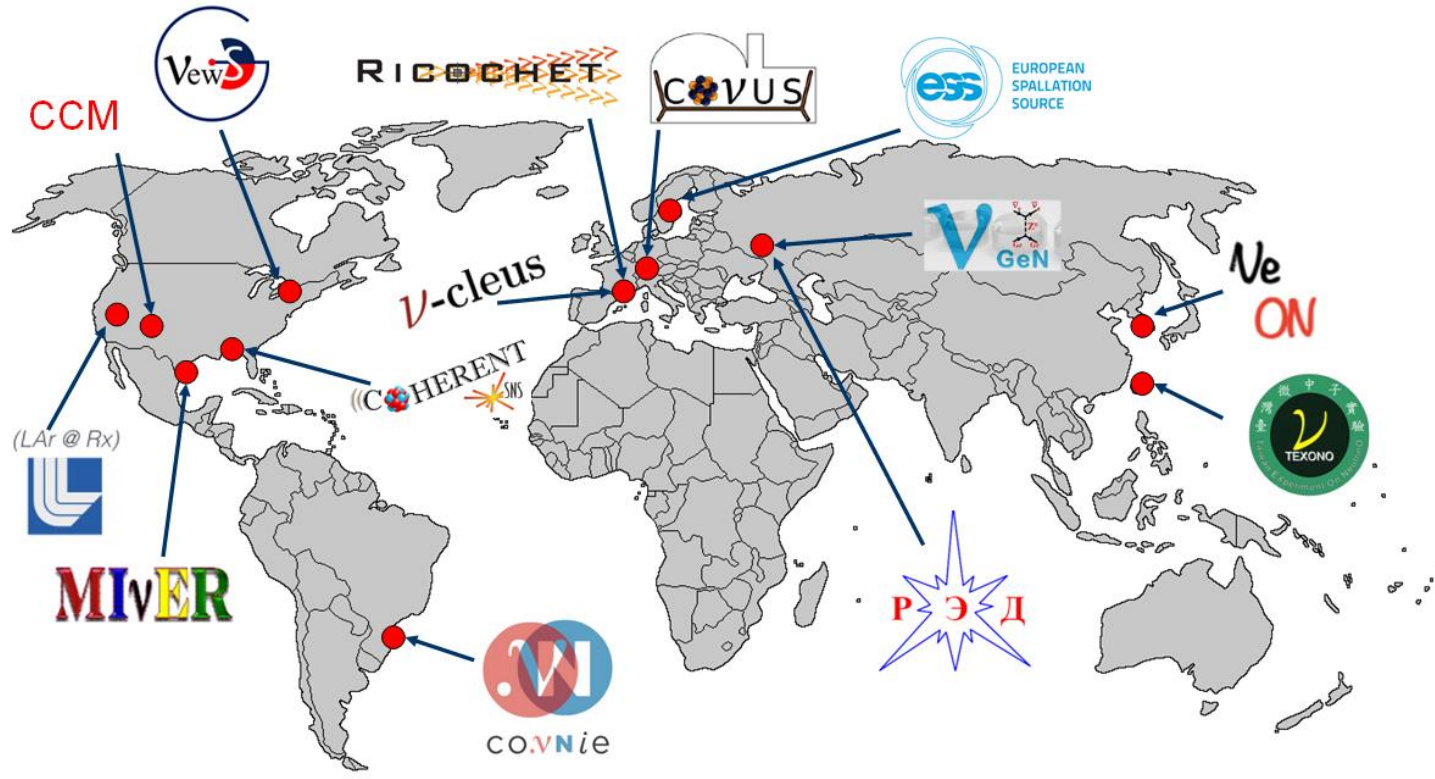
Alexey Konovalov (ITEP, MEPHI)



20 institutions from 4 countries (USA, Russia, Canada, S. Korea)

COHERENT uses the SNS facility neutrino source (ORNL)

The main goal is to look for new physics using coherent elastic ν -nucleus scattering

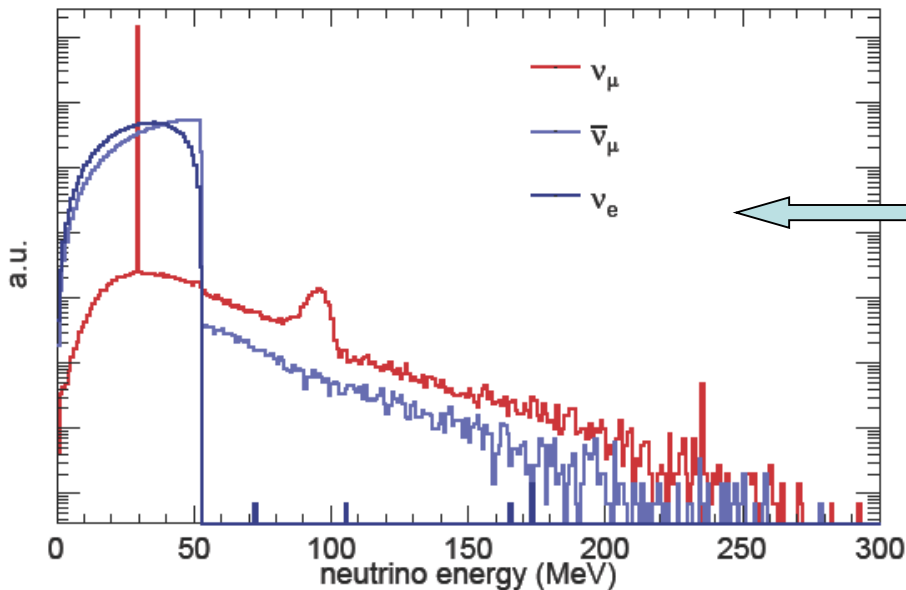
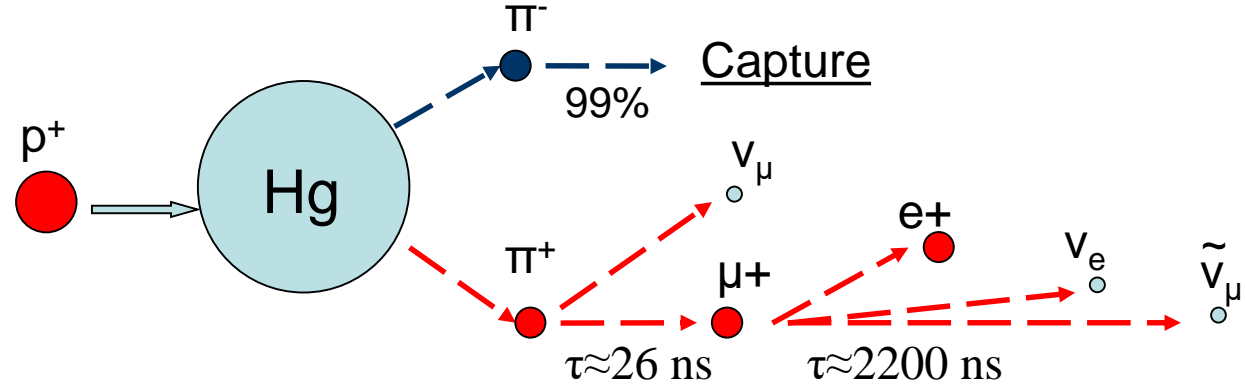
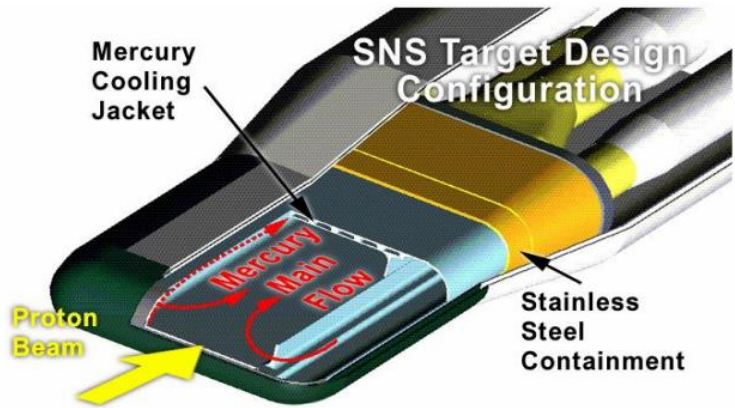


CEvNS search and study experiments around the world

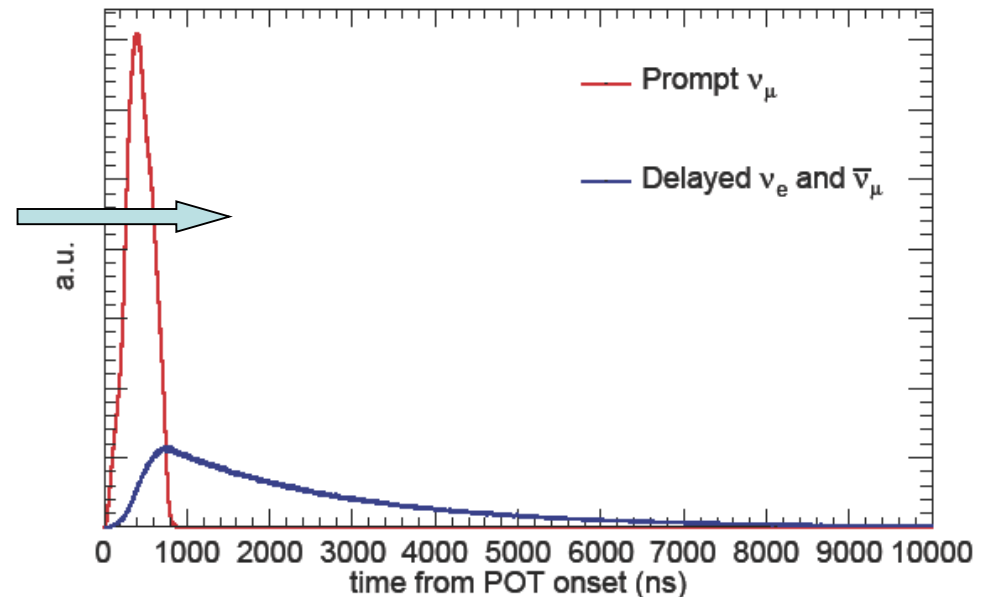
Bunches of ~ 1 GeV protons on the Hg target with 60 Hz frequency

Proton bunch time profile with FWHM of ~ 350 ns

Total neutrino flux of $4.3 \cdot 10^7 \text{ cm}^{-2} \cdot \text{s}^{-1}$ at 20m



ν energy and timing suit well for CEvNS search

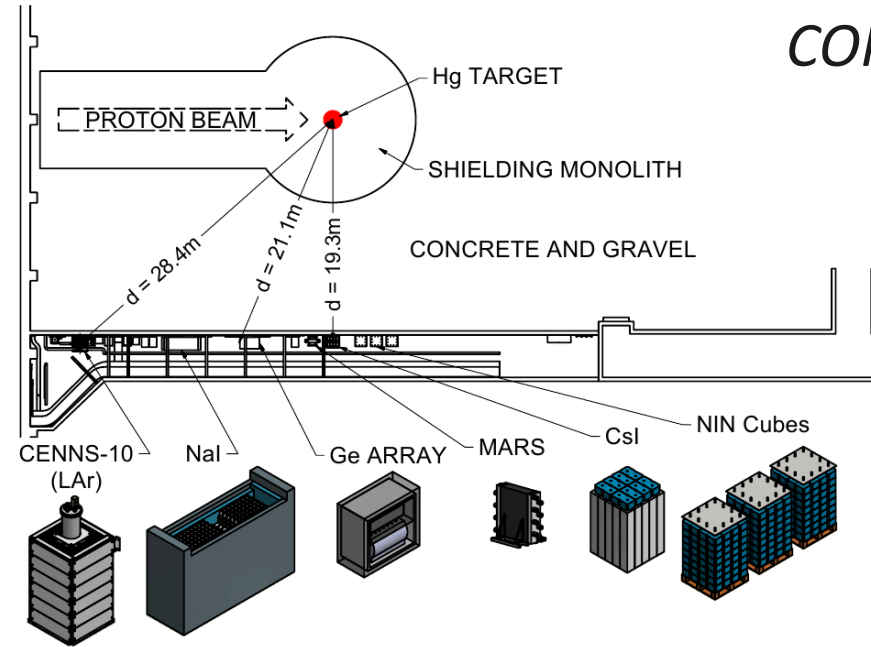


COHERENT detectors are hosted by the target building basement

20 m of steel, concrete and gravel with no voids in the direction of the target

8 MWE vertical overburden

Large background suppression comes from the construction materials and beam timing



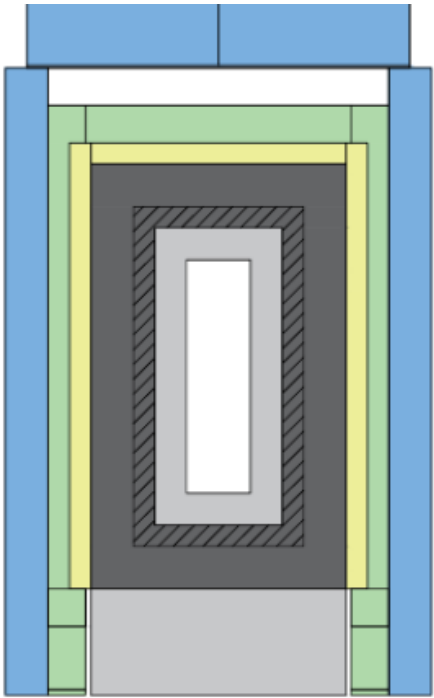
Multiple detectors complement each other in a chase for rich physics

Topic	CsI	Ar	NaI	Ge	Nubes	D ₂ O
Non-standard neutrino interactions	✓	✓	✓	✓		
Weak mixing angle	✓	✓	✓	✓		
Accelerator-produced dark matter	✓	✓	✓	✓		
Sterile oscillations	✓	✓	✓	✓		
Neutrino magnetic moment		✓	✓	✓		
Nuclear form factors	✓	✓	✓	✓		
Inelastic CC/NC cross-section for supernova		✓			✓	✓
Inelastic CC/NC cross-section for weak physics		✓	✓		✓	✓

The sum is greater than the individual measurement
 All measurements benefit from neutrino flux normalization

The status and future of COHERENT detectors will be covered in the talks by *D. Pershey* and *J. Daughetee*

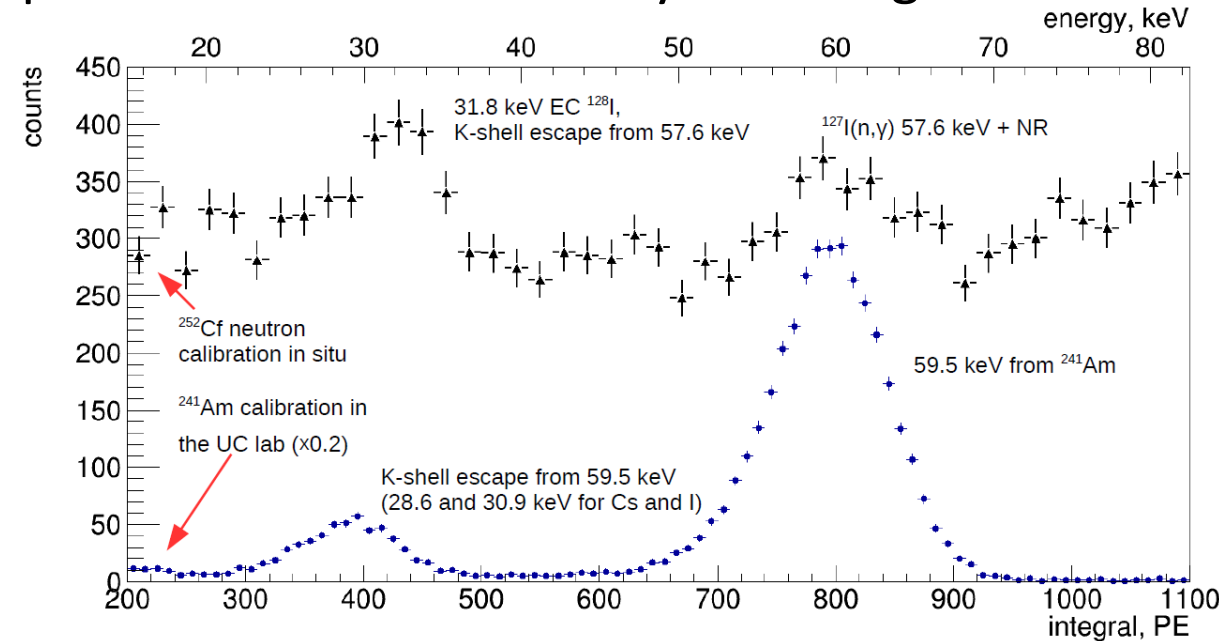
Crystal manufactured by Amcrys-H, Ukraine; set up created in the University of Chicago






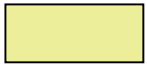

<i>Length</i>	<i>34 cm</i>
<i>Diameter</i>	<i>11 cm</i>
<i>Weight</i>	<i>14.6 kg</i>

Read out by single R877-100 PMT

Light yield of the crystal is ~ 13.3 PE/keV and it's uniform within 3% across the crystal length



Shielding design

Layer	HDPE	Low backg. lead	Lead	Muon veto	Water
Thickness	3"	2"	4"	2"	4"
Colour					

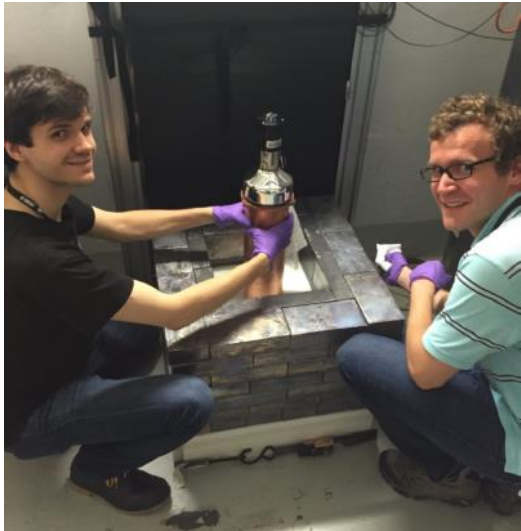
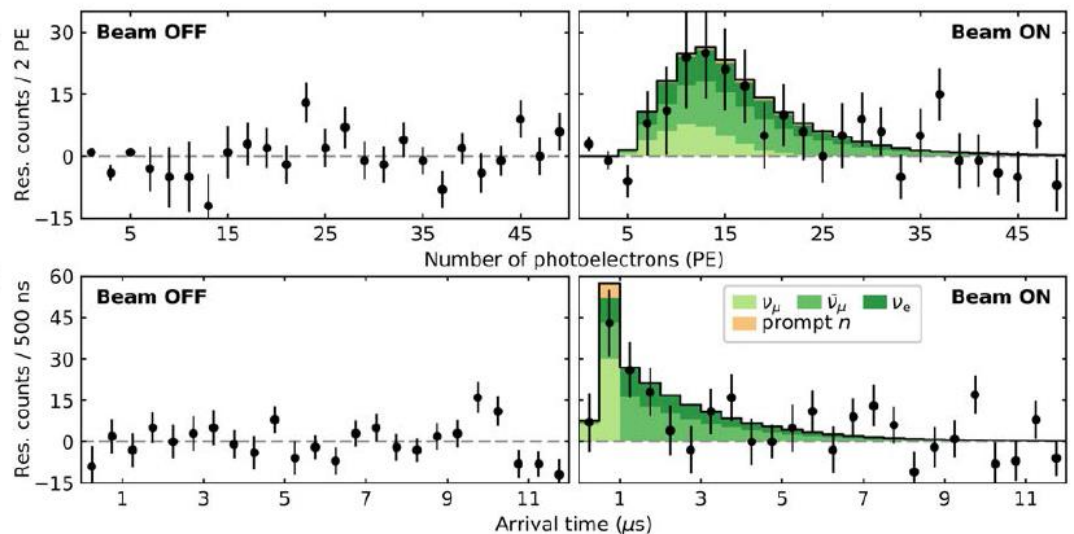
More information in

J. Collar et al., NIM A773, 56 (2015)

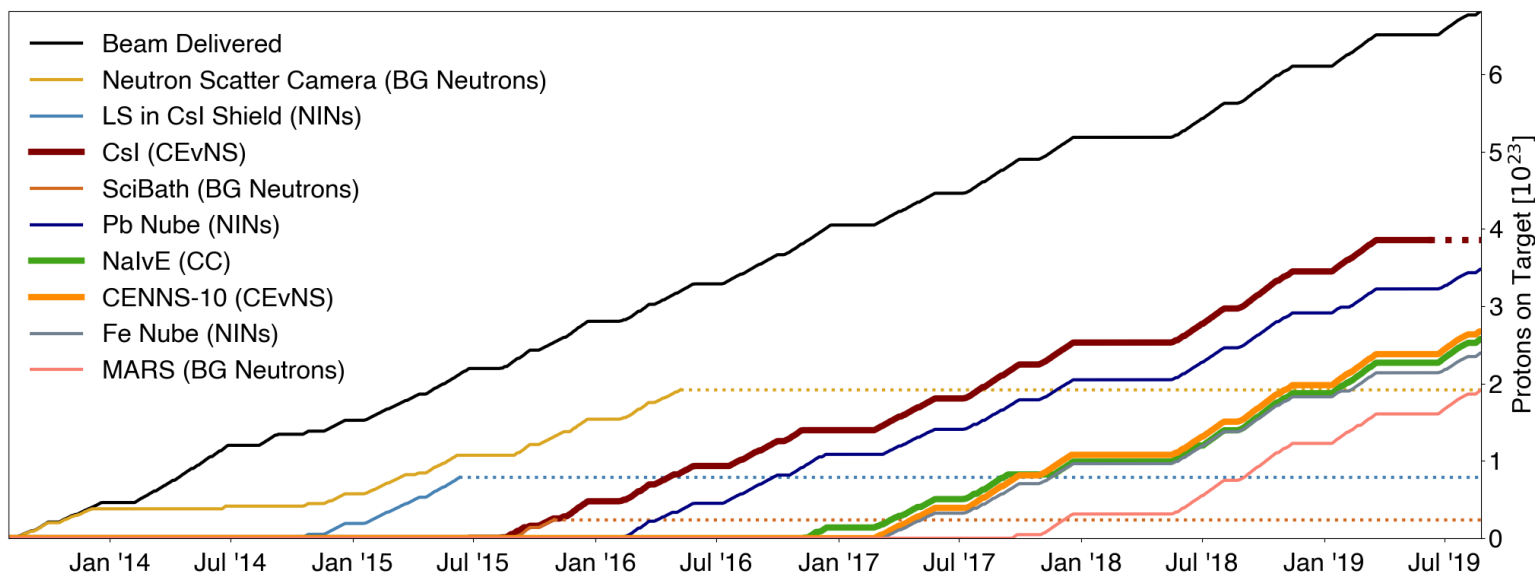
B.J. Scholz PhD thesis (2017)

6.7 σ significance result was reported in 2017, 43 years after prediction

D. Akimov et al., *Science* vol. 357 (2017),
 B.J. Scholz (U.Chicago) thesis (2017),
 G.C.Rich (NCU) thesis (2017)

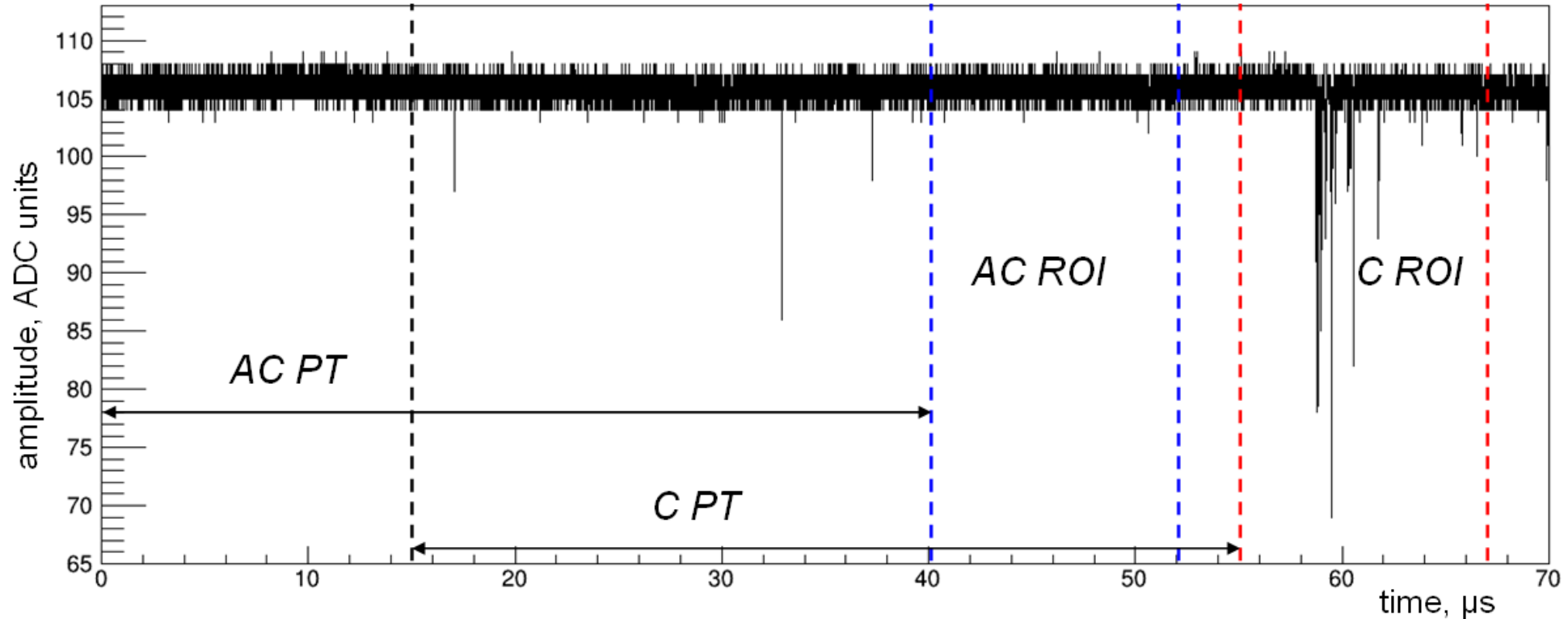


Data taking continued up to June 10 2019, then detector was decommissioned



More than 2x statistics is available now relative to the 2017 dataset

We acquire 70 μs waveform traces based on the external “POT” signal with no hardware threshold



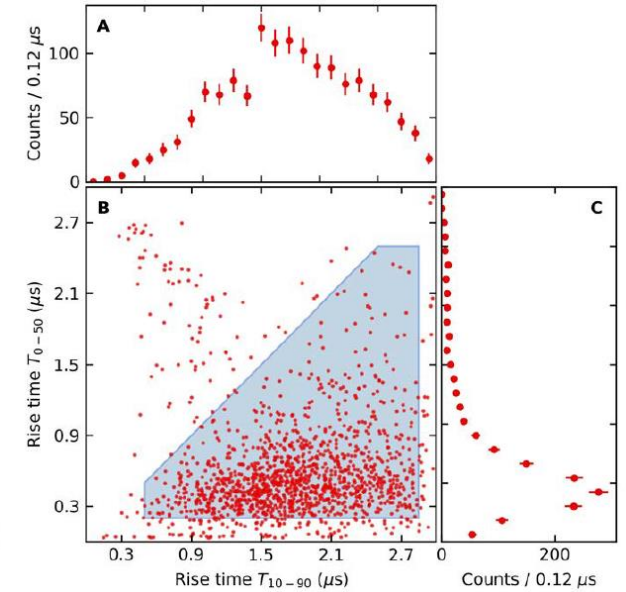
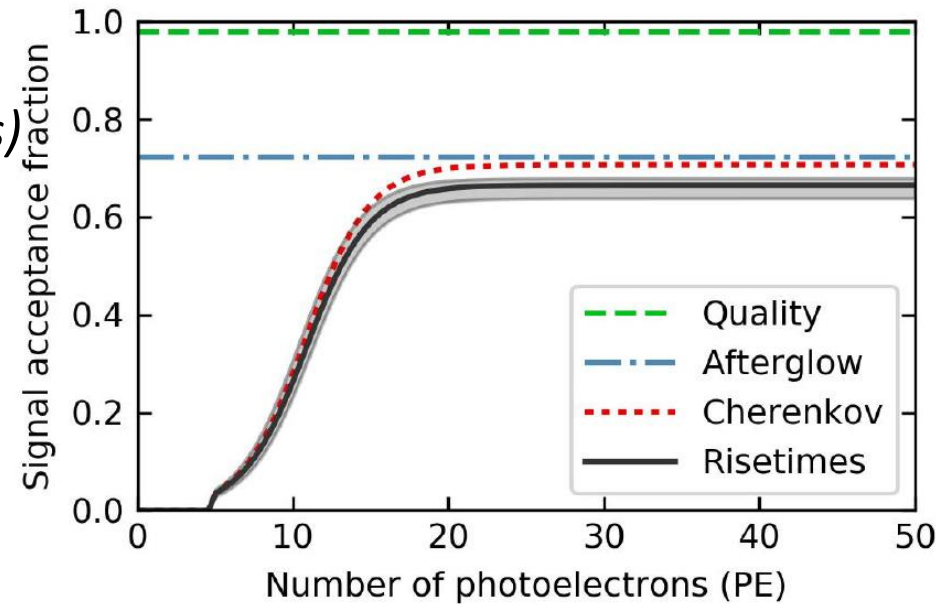
We look at two regions (ROIs) – coincidence (C) and anti-coincidence (AC), residual spectra of signals' integral and arrival time correspond to beam-related interactions. Each ROI is preceded by pretrace (PT).

Signal onset - first pulse (PE) in the ROI, integral is calculated within [onset, onset+3 μs]

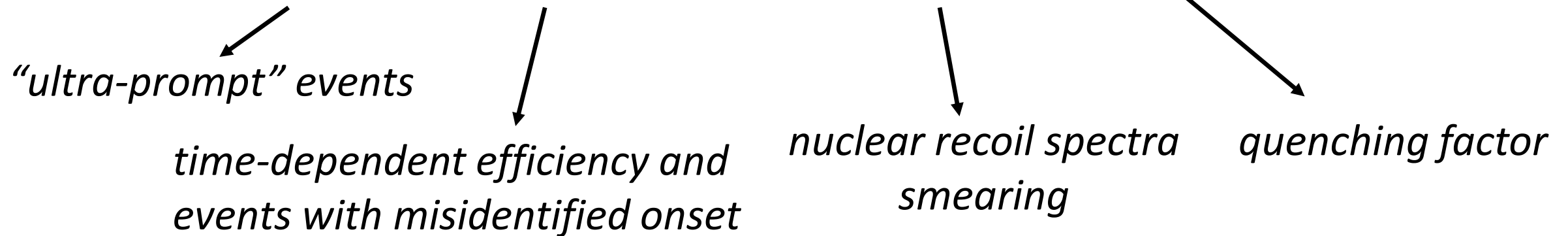
From D. Akimov et al., Science vol. 357 (2017), B.J. Scholz (U.Chicago) thesis (2017)

Cuts summary:

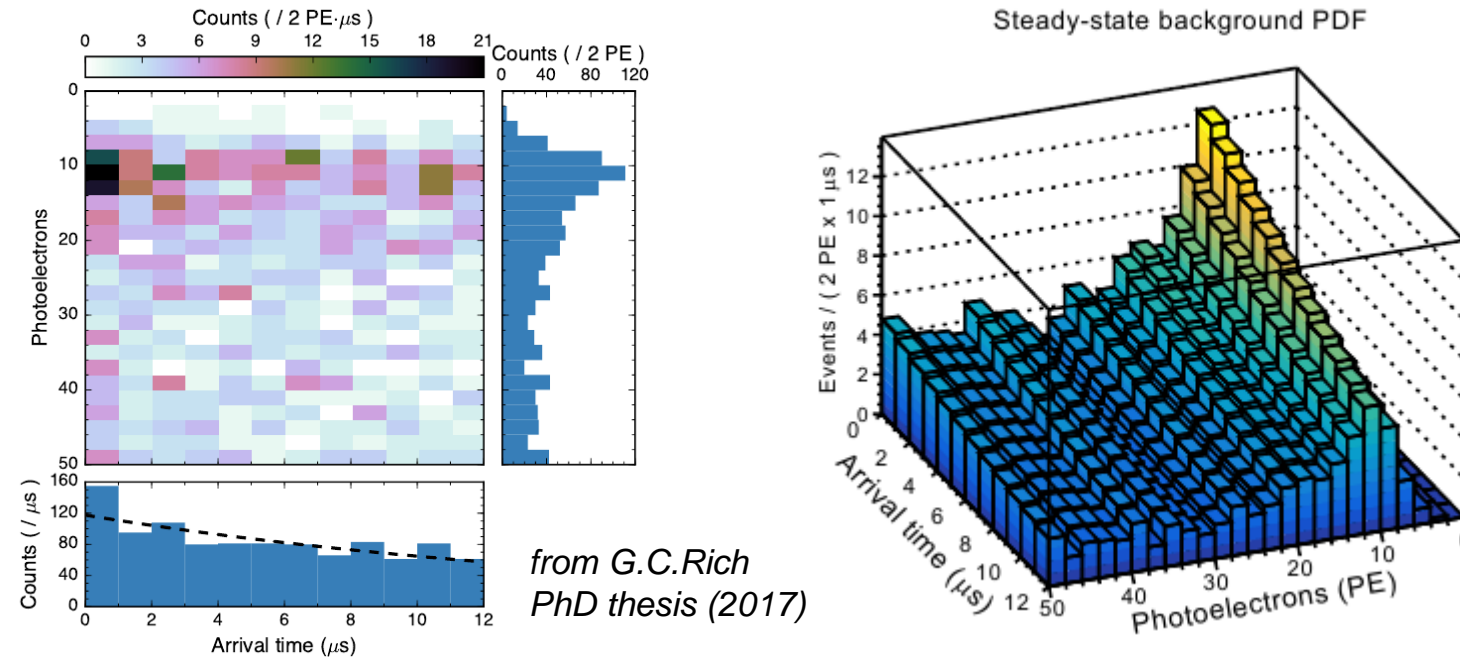
1. Quality (muon veto, ADC range issues)
2. Afterglow ($N_{PT} \leq 3$) – pulses in PT
3. “Cherenkov” ($N_{ROI} \geq 8$) – pulses in ROI
4. Risetimes (T_{0-50} , T_{10-90})



Investigation of systematics and new features in the CsI[Na] data analysis

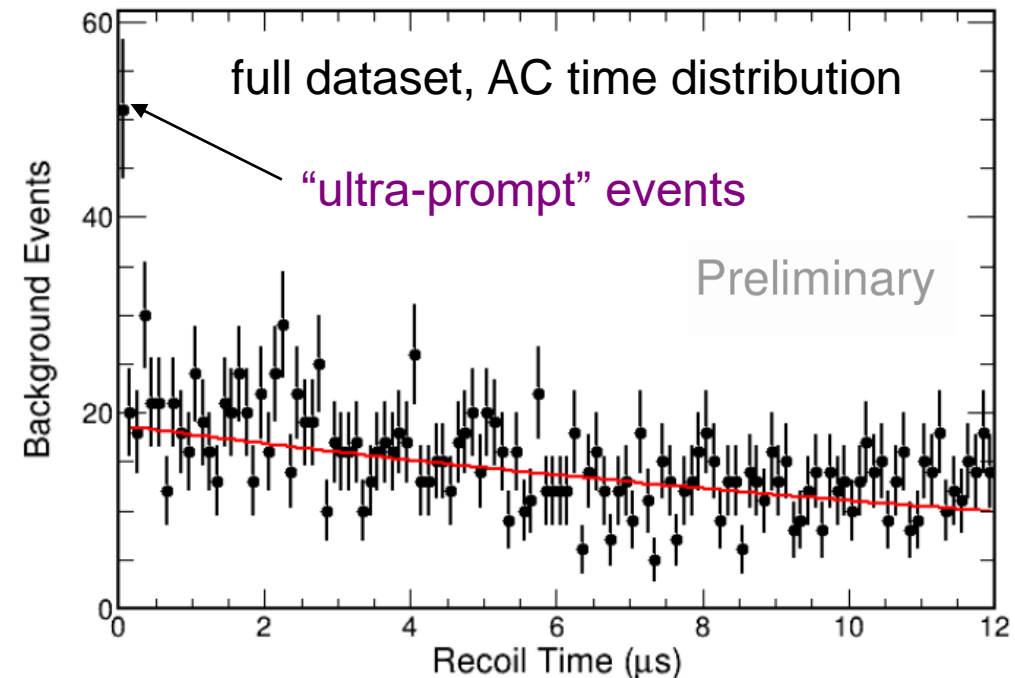


We use integral and timing information from the AC events to construct the background PDF. In the case of interaction-induced events integral and arrival time are independent, PDF is factorized.



Finely sampled data show deviation from the exponential model in the first 100ns.

Artificial excess in the first 100 ns would be observed for (data-model) “as is”

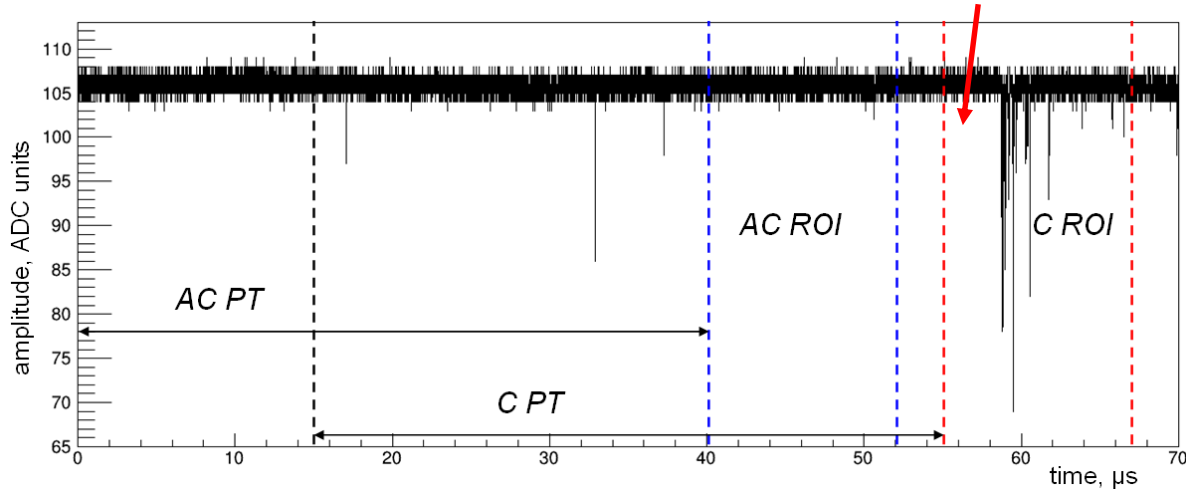


It turns out that low energy signals having few PE in PT pass the cuts on the number of pulses in PT and are accepted as ROI events

For this analysis we require no pulses in the latest 200 ns of PT which suppress the number of ultra-prompt events from ~ 40 to ~ 1 , which is much lower than uncertainty in the total BG rate

We also require no “large” (>10 PE) signals in PT which removes large continuous signals spilling over to ROI

What happens if an afterglow pulse appears here?



Misidentified onset

$\Delta t(\text{afterglow-signal}) < 3 \mu\text{s}$
 “messed up” – distorted timing and integral info

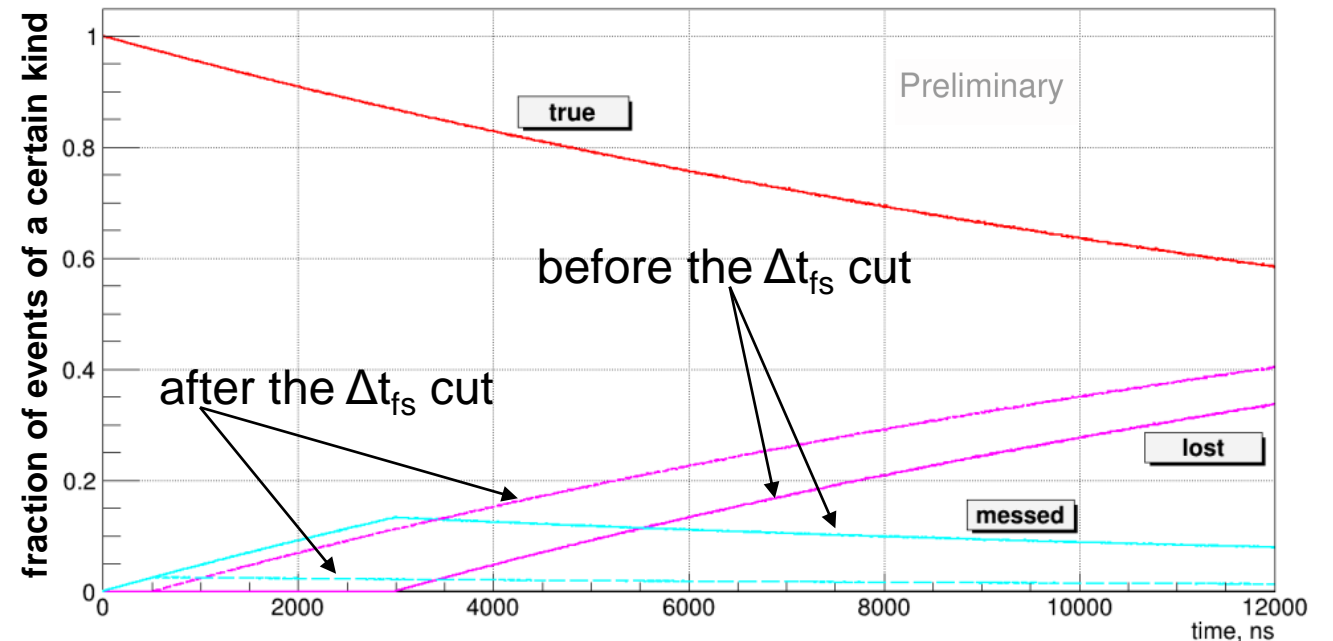
$\Delta t(\text{afterglow-signal}) \geq 3 \mu\text{s}$
 “lost” – event doesn’t make it to the spectra

We utilize the time delay between the first and the second pulse Δt_{fs} ($\leq 520\text{ns}$) in the signal to suppress contribution from “messed up” events by the factor of ~ 5

In 2017 the problem of “messed up” events was addressed by risetime cuts, but the time-dependency and existence of “lost” events was not taken into account.

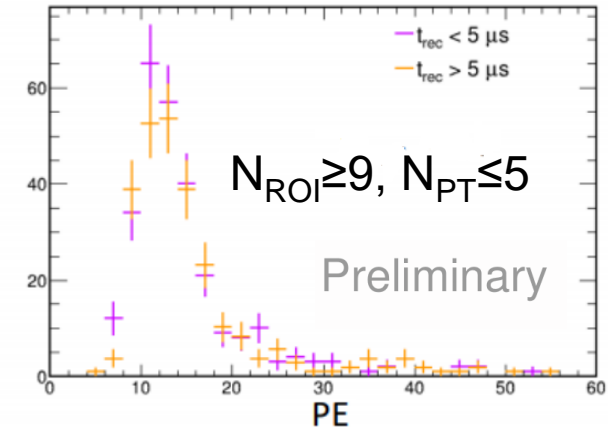
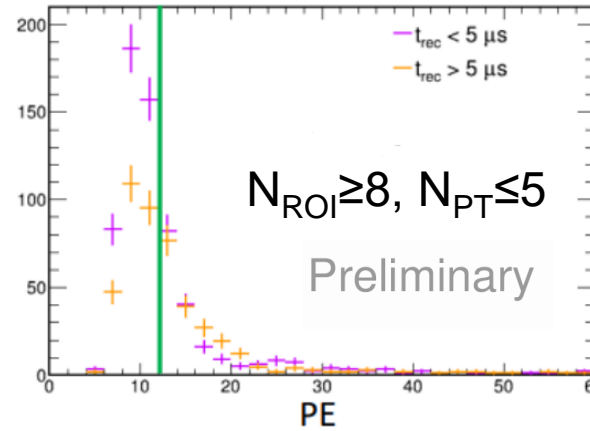
We don’t use risetime cuts in this version of analysis

Simulation based on the AC events first pulse appearance



We use a cut on the number of pulses in the signal N_s (“Cherenkov” cut). We used $N_s \geq 8$ in the 2017 analysis.

AC data for N_{ROI} cuts below $N_{ROI} \geq 9$ show deviation from the expected independency between time and integral
 “Prompt” BG component have more low integral events than “delayed” part (normalized by a total integral in each)

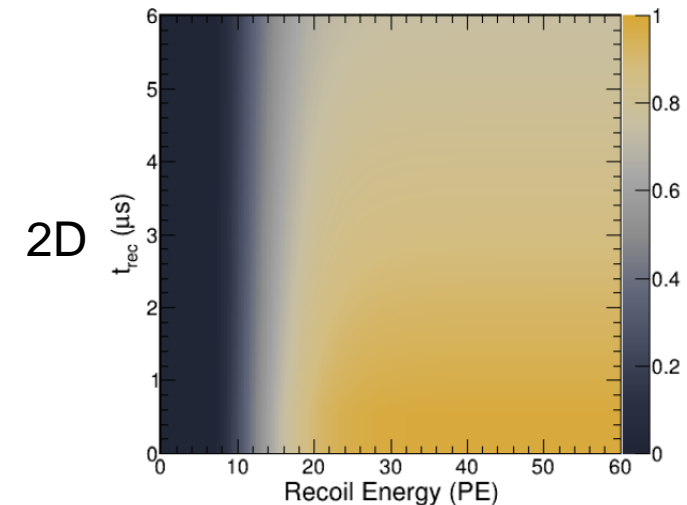
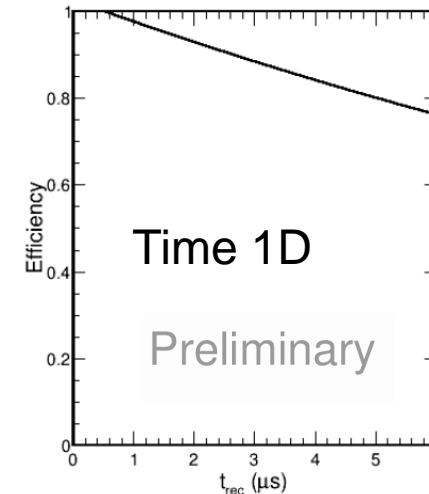
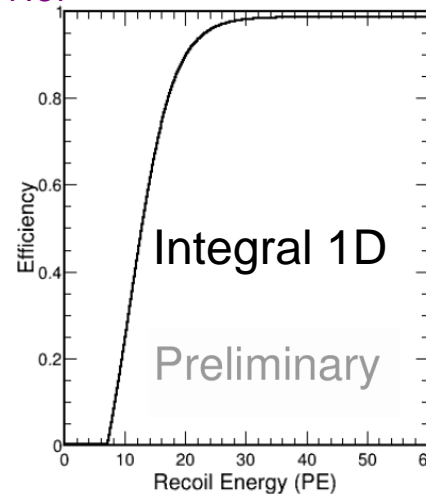


The reason – signals from the random coincidence of afterglow pulses within $3 \mu s$ integration time. They tend to have “earlier” arrival time relative to regular interaction-induced events (higher local afterglow rates contribute)

In this analysis we use $N_{ROI} \geq 9$ Cherenkov cut to avoid bias connected to the integral-time conspiracy in the AC data. Pretrace cut $N_{PT} \leq 5$ is an optimal pair for $N_{ROI} \geq 9$.

Final efficiency:

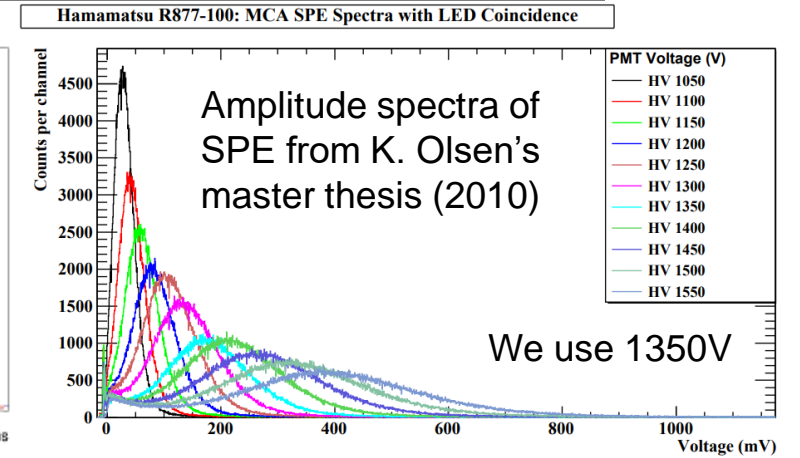
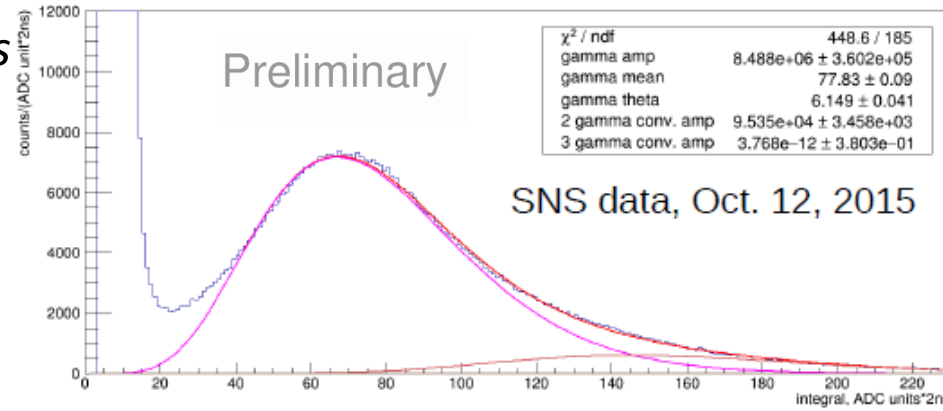
$$\varepsilon(\text{PE}, t_{rec}) = \varepsilon_E(\text{PE}) \times \varepsilon_t(t_{rec})$$



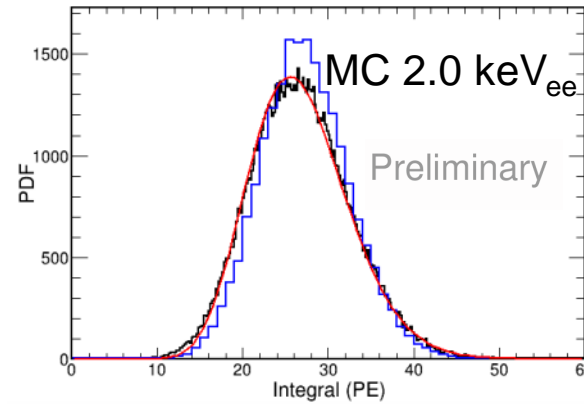
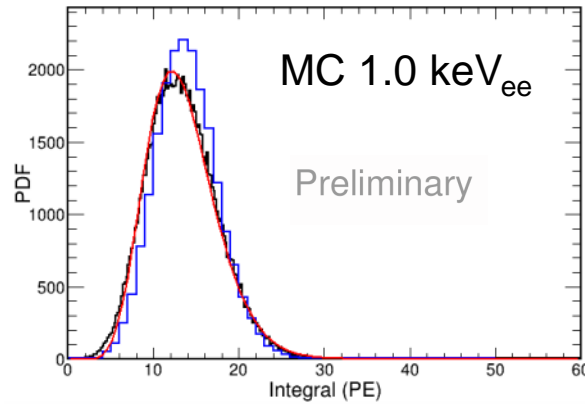
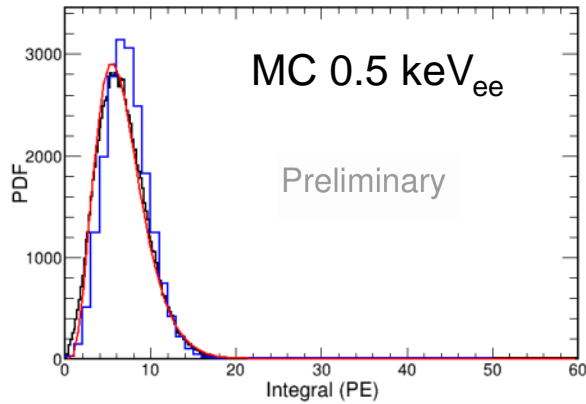
We use Polya/gamma distributions for tracking of the SPE charge

J.R. Prescott, NIM 39.1 (1966)

P.A.Amaudruz et al., NIM A 922 (2019)



Since the SPE integral spectrum RMS/mean ≈ 0.5 we can't ignore smearing contribution induced by SPE shape



Blue – pure photostat.

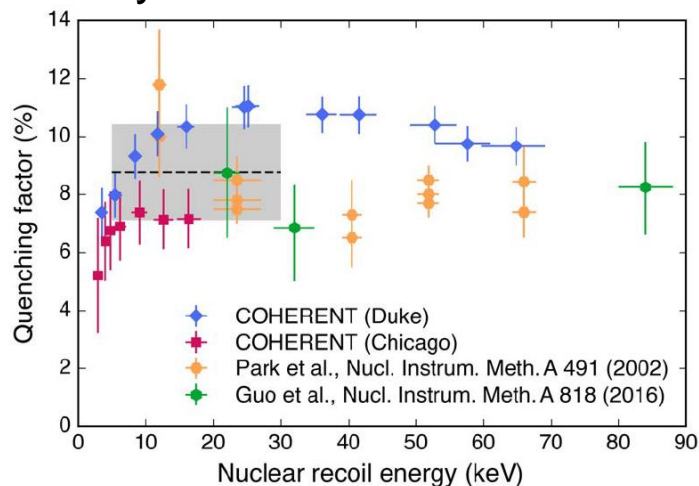
Black – photostat.+SPE

Red – gamma fit of result

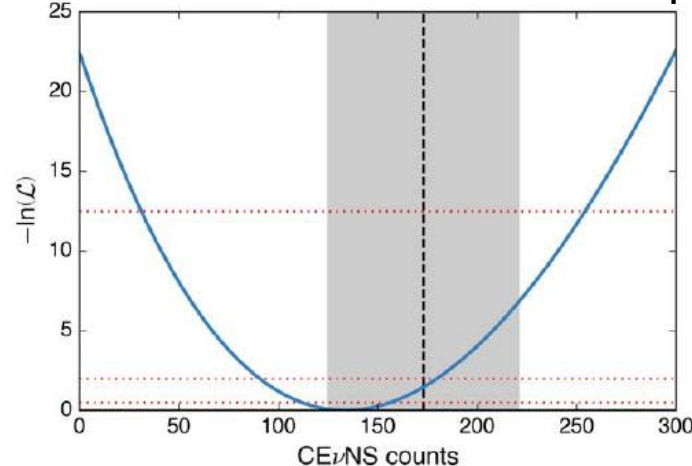
Smearing is empirically parameterized by gamma distribution $P(x) = \frac{(a(1+b))^{1+b}}{\Gamma(1+b)} x^b e^{-a(1+b)x}$ with $a = \frac{1}{x}$ and $b = 0.7157 \times x$

At the time of the first CEvNS observation (2017) the QF value uncertainty dominated the prediction uncertainty

Gray marks $8.8 \pm 1.7\%$ value



134 ± 22 observed vs. 173 ± 48 predicted

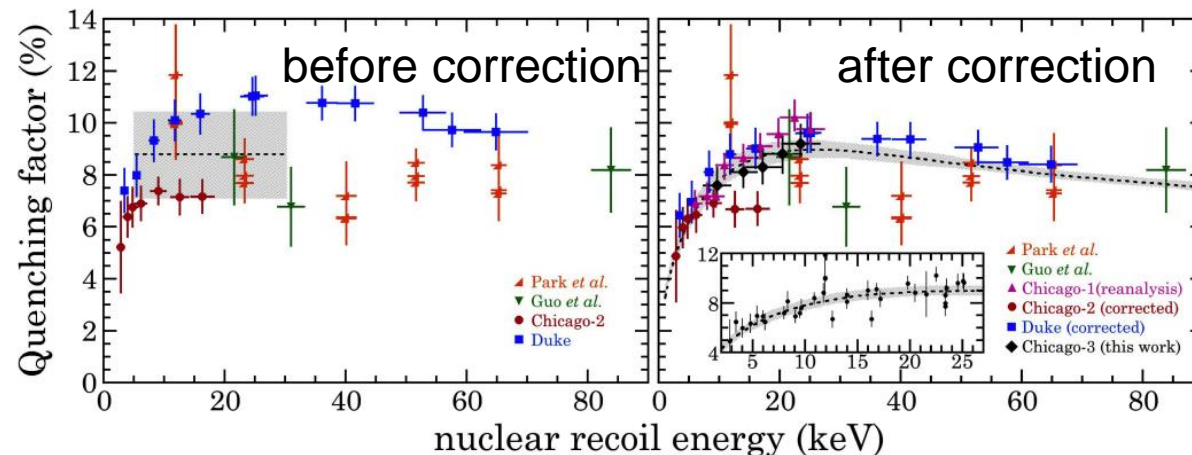
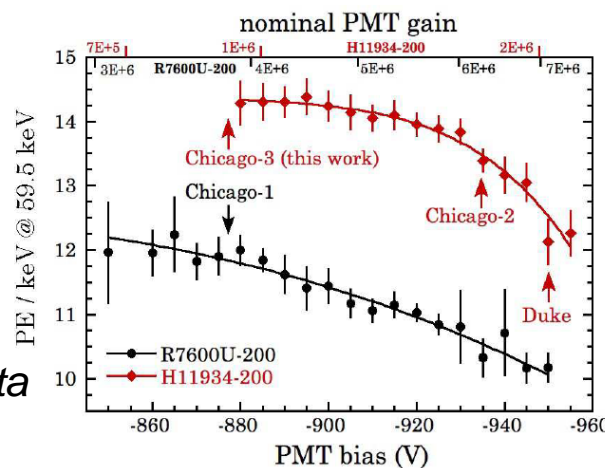


The uncertainty was estimated by discrepancy in results of two measurements by COHERENT

Over the following years there were Prof. J. Collar's and COHERENT updates on QF values issue

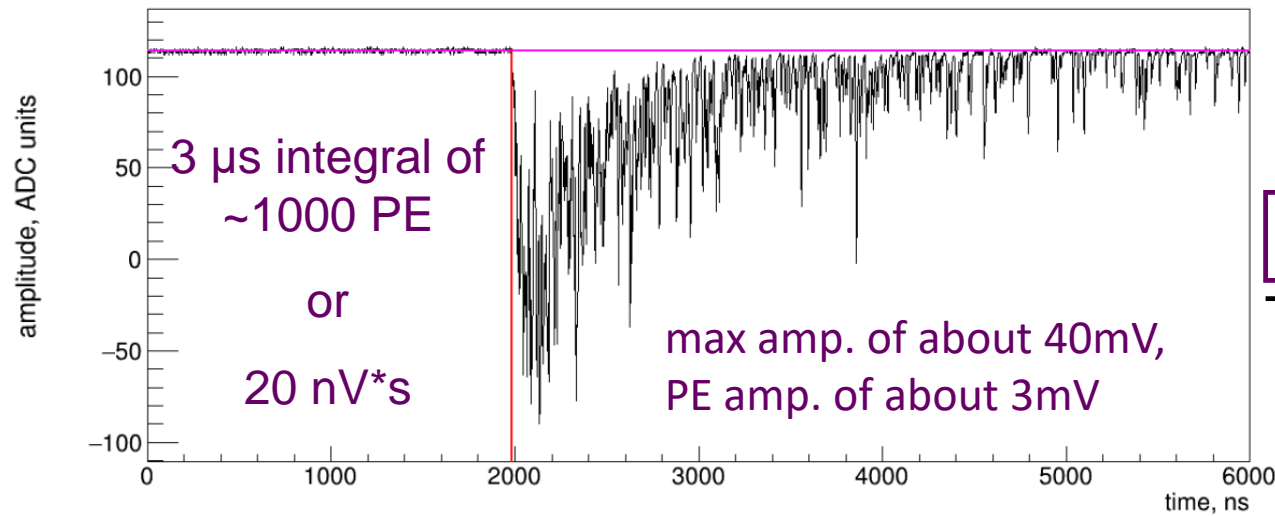
J. Collar et al., PRD 100 (2019):

1. New Chicago-3 data
2. Re-analysis of Chicago-1
3. PMT non-linearity claim and corrections to COHERENT data



Scale of the 59.5 keV signals in COHERENT-2 measurement (-935V)

Crude estimate from the manufacturer's info



Let it be 1200 PE signal from the PMT at -950V

Let the gain be $2 \cdot 10^6$ at 950V (from the manufacturer info)

$$2.4 \cdot 10^9 \text{ e} \approx 4 \cdot 10^{-10} \text{ C}$$

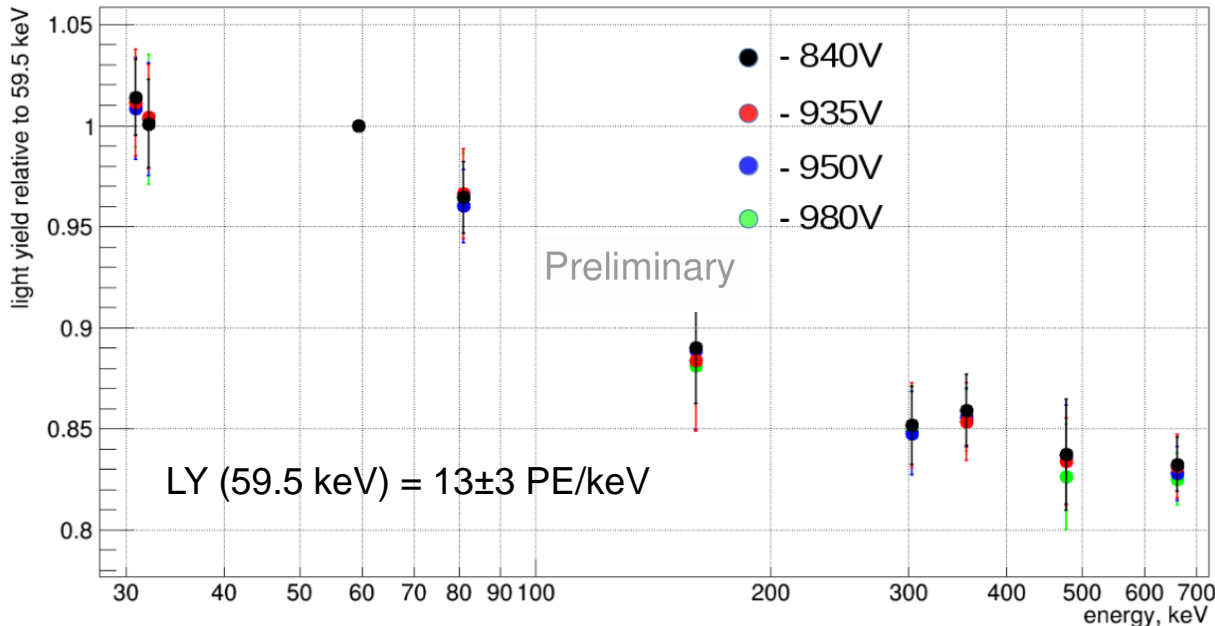
$$300 \text{ ns (vs. } 3 \mu\text{s)}$$

$$= 1.3 \text{ mA}$$

vs. $\pm 2\%$ at 20mA

from Hamamatsu info

Tests with the crystal – relative light yield



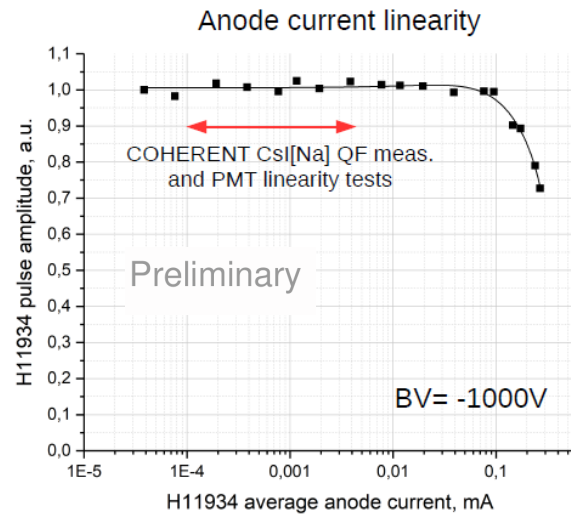
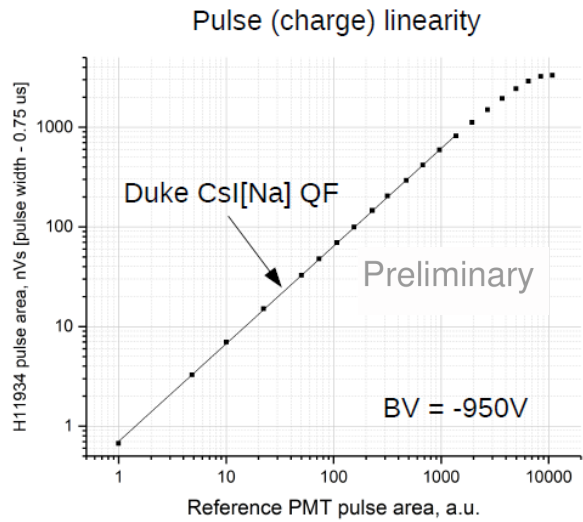
No change in the rel. LY in 840V-980V bias voltage for the lines in [30, 662] keV energy range

Change in the rel. LY with energy comes from the CsI[Na] non-linearity and is consistent with the literature

G. K. Salakhutdinov et al., Instr. Exp. Tech. 58 (2015)

W. Mengesha et al., IEEE TNS 45 (1998)

P. R. Beck et al., IEEE TNS 62 (2015)



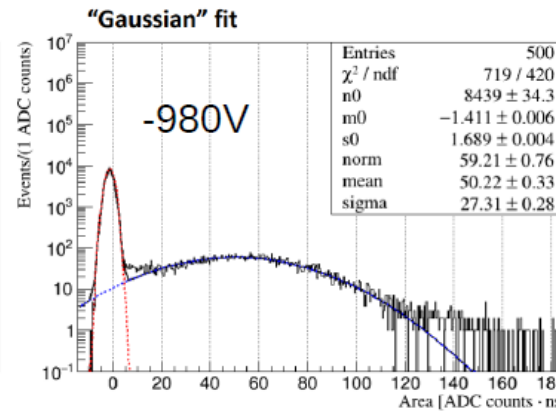
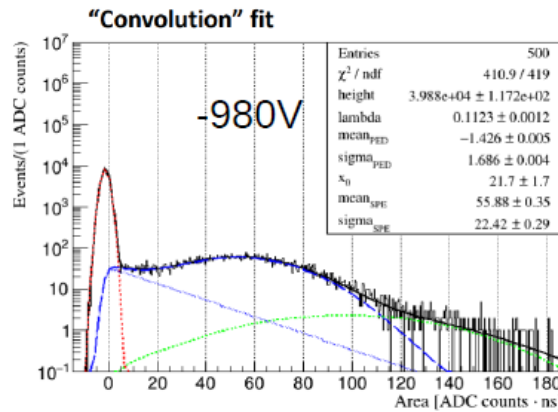
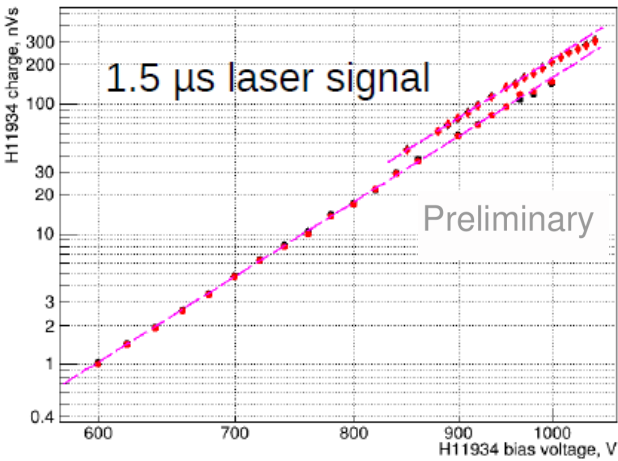
The test of H11934-200 vs. the reference FEU-143 suggests the charge non-linearity scale at $\sim 1000 \text{ nV}\cdot\text{s} / 0.75 \mu\text{s} \rightarrow 30 \text{ mA}$, which is close to manufacturer's info ($\pm 2\%$ at 20 mA, $\pm 5\%$ at 60 mA)

Linearity in the signal ROI scale is also confirmed by the two pulse method in 935-1000V within 4%

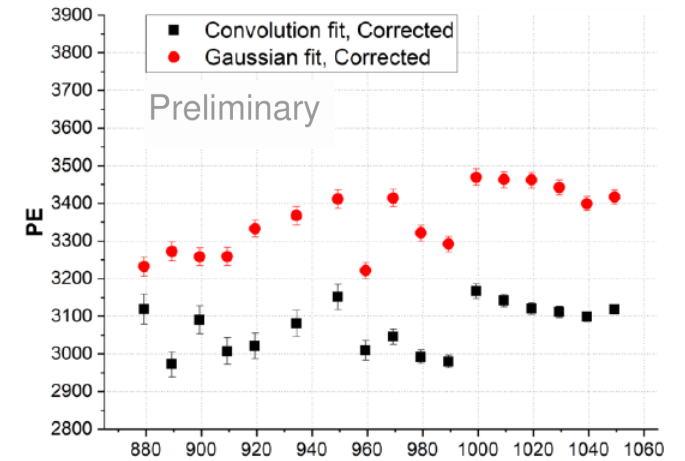
COHERENT data are not affected by the anode current non-linearity either

Thanks to Yu. Melikyan (INR RAS) for help

Fixed integration window SPE integration with a digital oscilloscope and 30 ps long laser pulse




Simple Gaussian model doesn't describe observed spectra



We refute the H11934-200 non-linearity claim with the PMT which was used for the measurements and don't agree with the corrections applied to QF measurements in [PRD 100 \(2019\) paper](#)


QF efforts on COHERENT side:

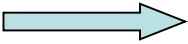
Cross-check confirms results of initial analysis, few corrections:

1. COHERENT-1(2017) cross-check 
ex. COHERENT (Duke)

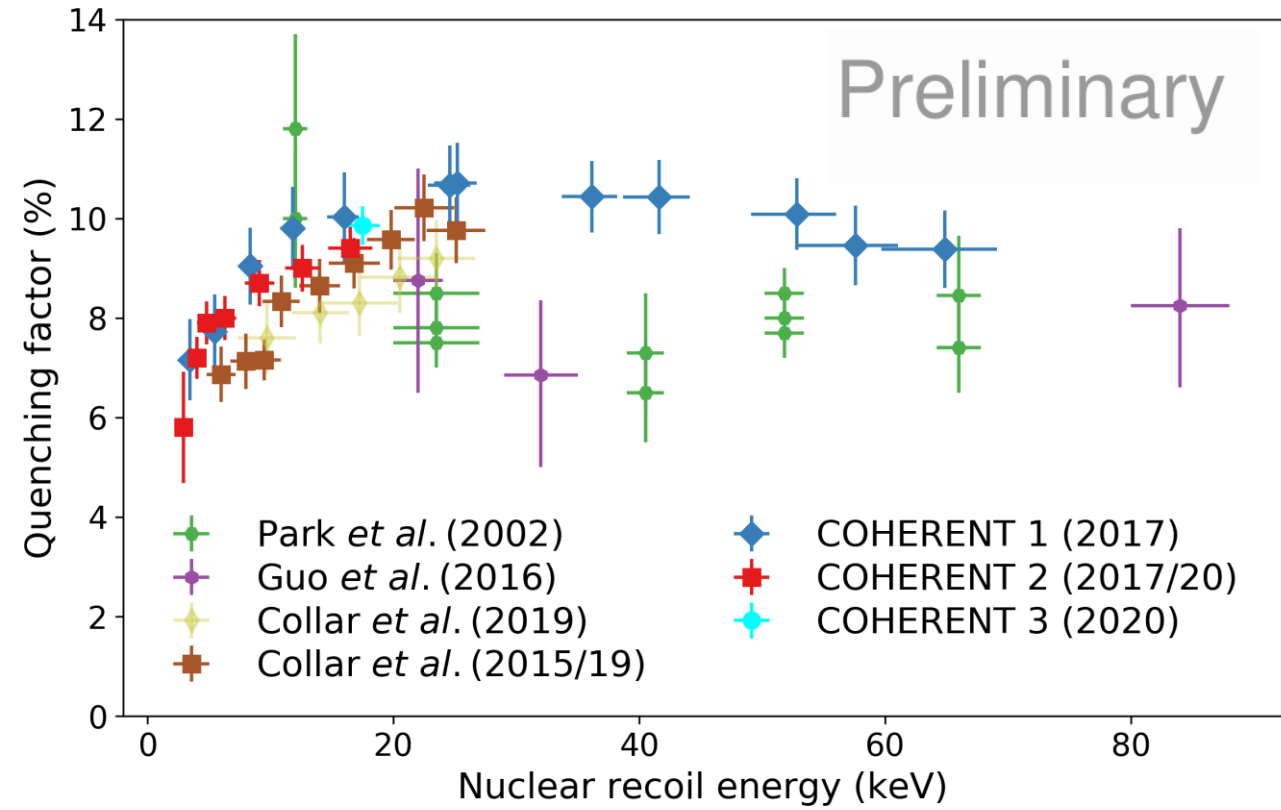
1. Issue in the energy calibration (-3% to QF values)

2. Mean afterglow contribution of 0.3PE – included in unc-ty

2. COHERENT-2 (2017)  *Cross-check doesn't confirm the initial results, full scaled re-analysis is performed*
Initial authors don't agree, but were not available for the joint re-analysis
ex. COHERENT (Chicago) / Chicago-2 in PRD 100 (2019)

3. COHERENT-3 (2020)  *Single ~17.5 keV NR energy measurement, QF = $9.86 \pm 0.40\%$*

4. COHERENT-4 (2020) [“The endpoint” measurement]  *No NR energy tagging, continuous NR spectrum for hypothesis test*



For the global QF fit we utilize data from:

Chicago-1 (2015/2019)

COHERENT-1 (2017)

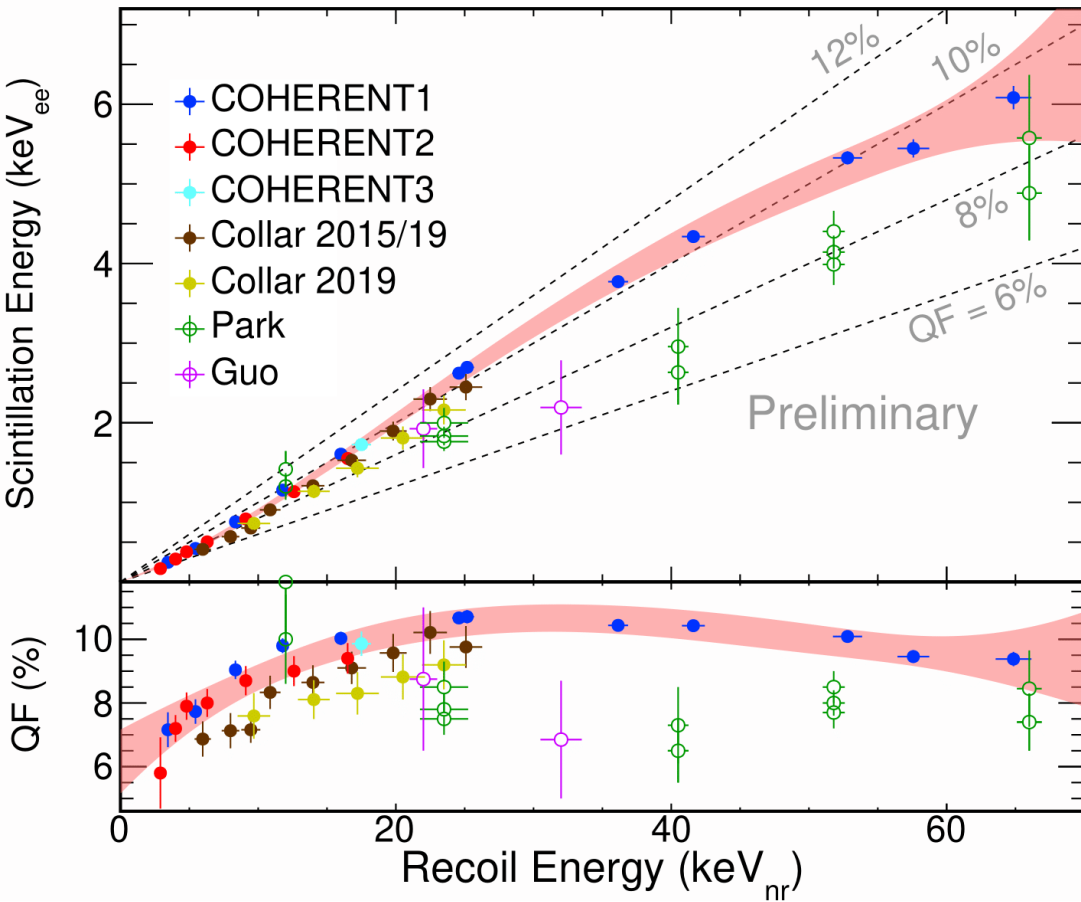
COHERENT-2 (2017/2020)

Chicago-3 (2019)

COHERENT-3 (2020)

all with the same small CsI[Na] crystal, produced by the manufacturer of the SNS crystal from the same

The global fit is performed in the “scintillation energy [keV_{ee}]” vs. “recoil energy [keV_{nr}]” to avoid double counting of E_{nr} uncertainty.

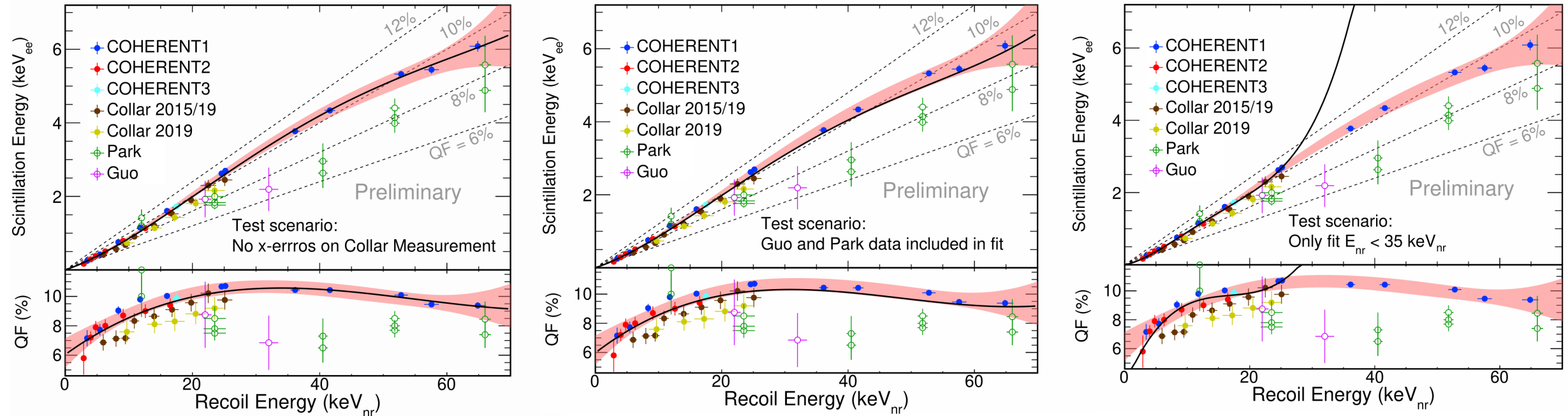


“Default” uncertainties:

1. No propagation of the NR energy spread into vertical uncertainty for COHERENT data
2. Chicago-1/3 data are taken with X-axis uncertainty from the *PRD 100 (2019)*, which is stated to be NR energy spread, zero X axis uncertainty is considered as systematic excursion

MCMC fit of the global data with 4th degree polynomial function, best fit (E_{nr} in MeV):

$$Sc(E_{nr}) = 0.0616006 \times E_{nr} + 3.37111 \times E_{nr}^2 - 77.9909 \times E_{nr}^3 + 519.958 \times E_{nr}^4$$



In order to address possible concerns the approaches to sharing of raw COHERENT QF data are discussed

We also will provide the summary table of existing measurements for use of community together with the data release

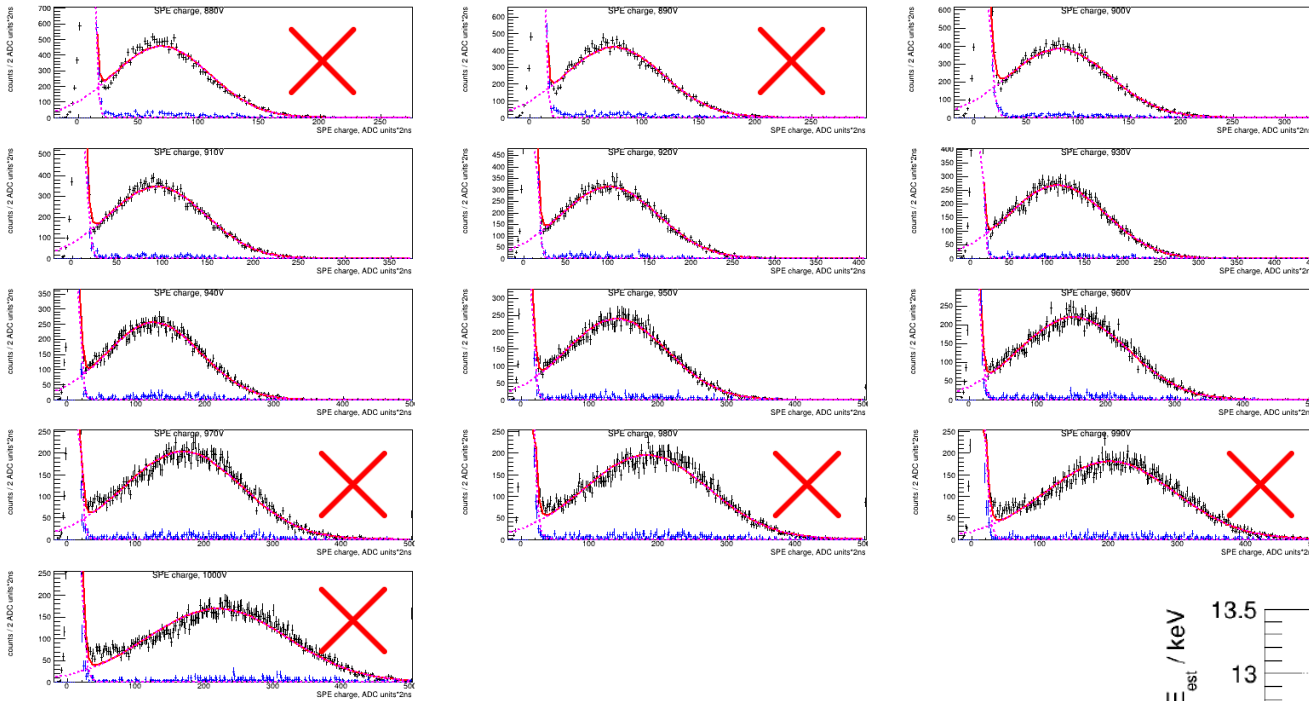
We addressed several issues in the steady-state background PDF evaluation making it more robust

- “ultra-prompt events” component is discovered and suppressed*
- “afterglow coincidence” component is understood and suppressed*
- time-dependent efficiency is included in the 2D PDFs of beam related signals*

We found and fixed an issue in the beam power database leading to the overestimate of cumulative BP/underestimate of observed CEvNS (7% effect)

We improved understanding of the CsI[Na] QF uncertainty reducing corresponding systematic uncertainty

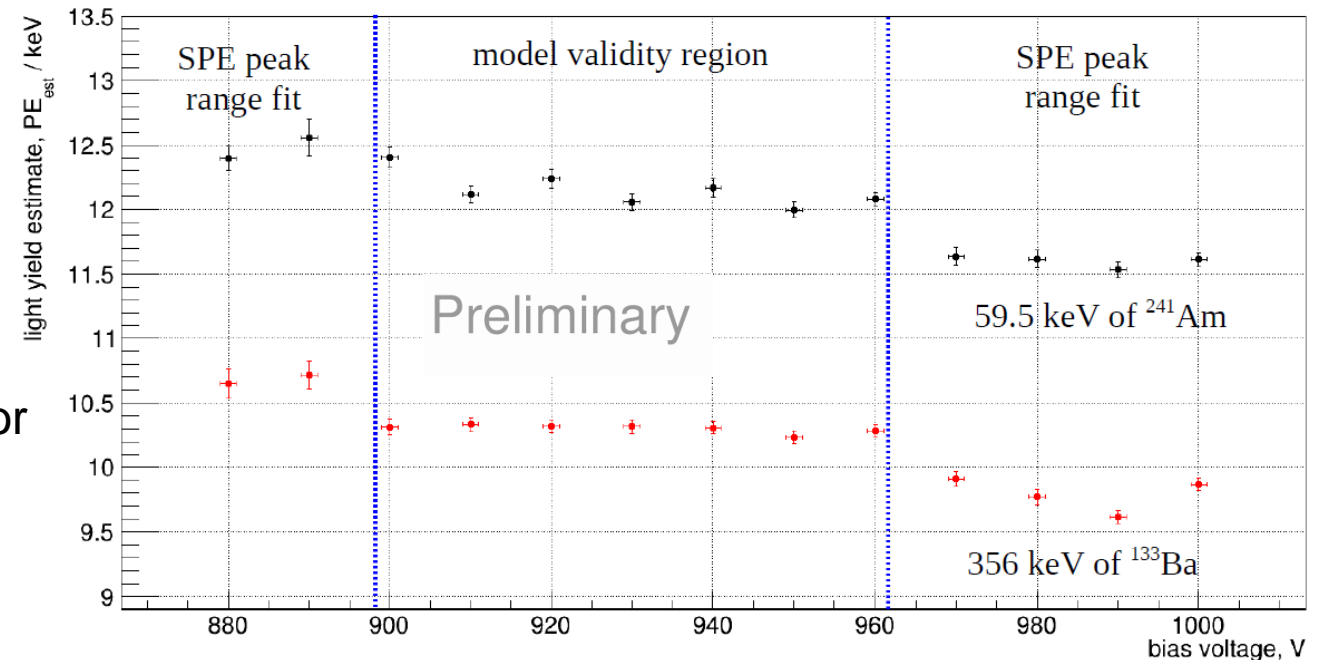
Thank you for your attention! The exciting results are just few steps away...



Gaussian SPE model fails at description of spectra at lowest (880-890V) and large largest (970-1000V) bias voltage

Non-gaussian shape of the distribution was confirmed in the laser pulse calibration of the PMT

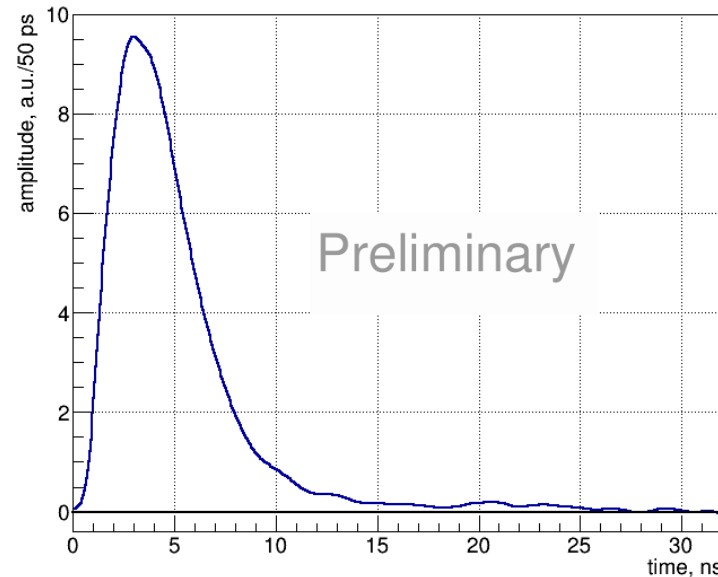
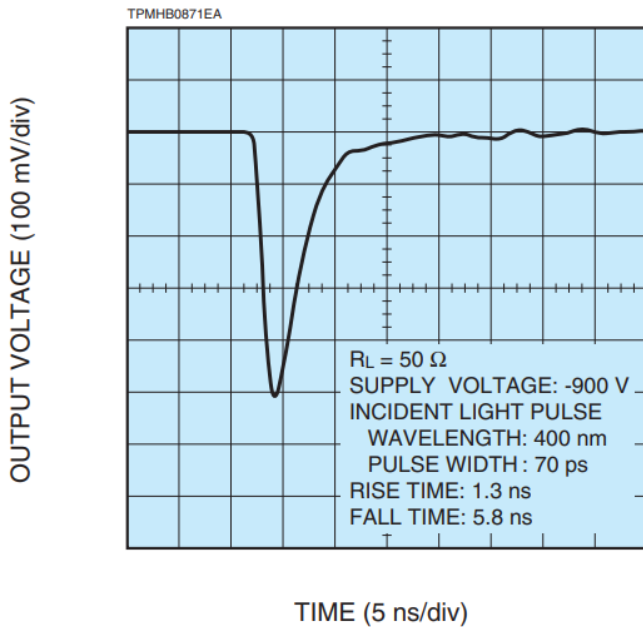
We don't observe the saturation-like behavior in the [900,960]V bias voltage range neither for 59.5 keV nor for 356 keV gamma line



1. H11934-200 SPE pulse shape and integration thresholds

Manufacturer's info

Our measurement with 30 ps laser pulse



Long low amp. tail may lead to the threshold effects in pulse finding approach depending on the signal/noise ratio sensitive to the PMT bias voltage

95% of integral are contained within 10 ns, 98% - 20 ns

We test our pulse finding procedures with artificial waveforms based on the SPE shape to check for potential under/over integration

2. Afterglow contribution

There's a chance that afterglow pulse accidentally sneaks into the NR signal integration window biasing the integrals to larger values – the average contribution is ~ 0.3 PE/ $3 \mu\text{s}$, but depends on the radiation load of a crystal. That's enough to bias the low NR energy QF by few to 10%.

COHERENT data either convolve afterglow contribution with MC prediction or expand unc-ty to take it into account

2. Binning of prediction

If Poissonian photostat. smearing is used to produce prediction based on the simulated NR energy spectrum, bin centers should be in the integer number of "PE" both for the prediction and the data. For a prediction spectrum in PE space with bin centers in non-integer PE values Poisson photostat. smearing redistributes counts to integer values -> lower bin edges which creates 0.5 PE between bias between obtained prediction (representative values stored at lower bin edge) and data (representative value of non-integer data stored at bin center).

3. Inelastic scattering n escapes contribution

In the act of inelastic scattering of neutron off nuclei sometimes high energy gamma is generated, this high energy gamma may escape the material sample generating single observable NR with distorted energy deposition. This effect is most noticeable at large scattering angles. Inelastic escapes contribution should be either included in prediction or suppressed by backing detector energy deposition/TOF.

COHERENT “The endpoint” measurement:

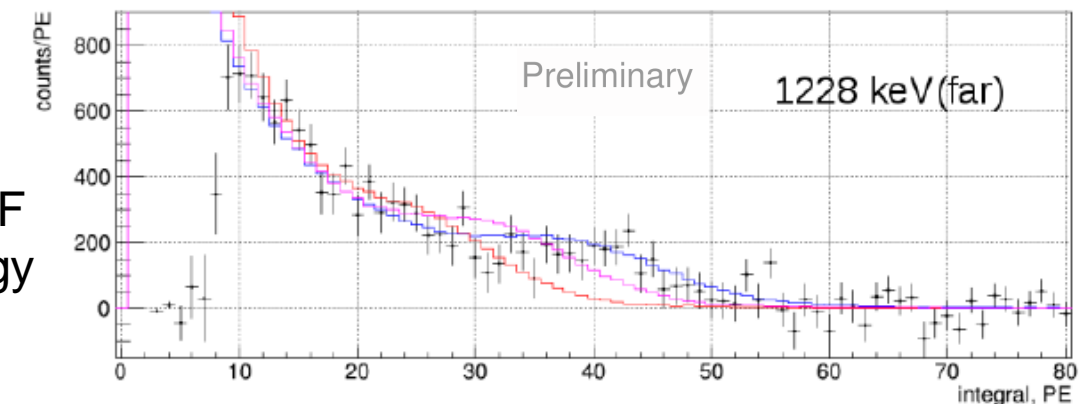
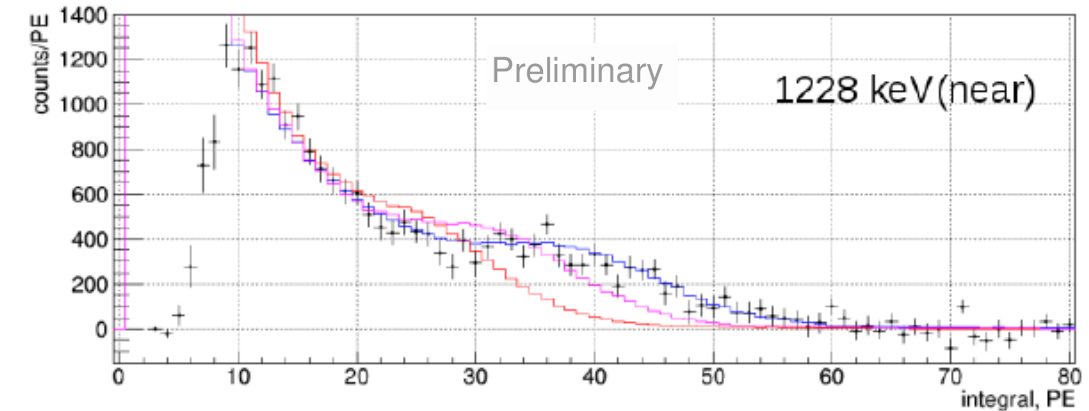
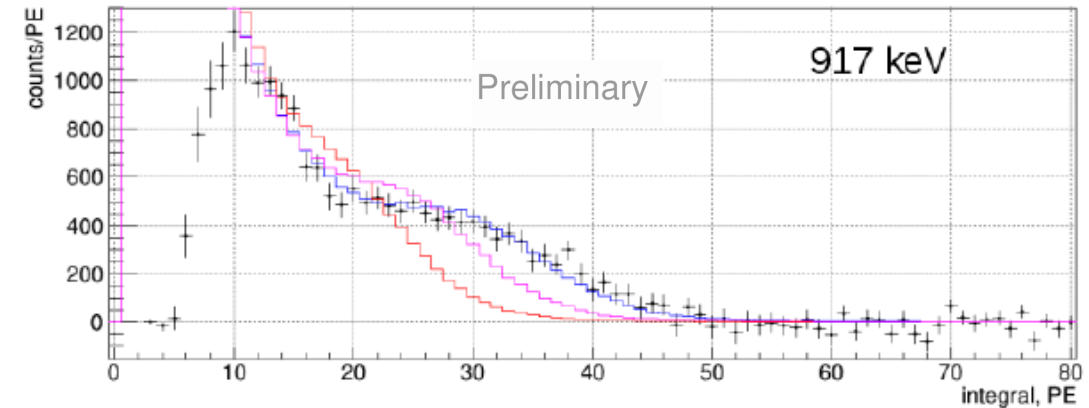
performed in TUNL with ${}^7\text{Li}(p,n){}^7\text{Be}$ source, two beam energies: 917 and 1228 keV identified by neutron TOF, two stand off distances for 1228 keV beam energy

The NR spectrum endpoints around 28 keV and 37 keV

The measurement can be used as a hypothesis test of QF data available in the literature:

1. Constant QF of 7.2% - red in the plots
2. J. Collar et al. (2019), best fit model – magenta
3. COHERENT-1 (2017) - blue

The reanalysis of COHERENT-2(2017) QF data suggests larger QF values, inconsistent with initial $\sim 7.2\%$ result in [6,17] keV NR energy



Plots from B.J. Scholz PhD thesis (University of Chicago), 2017

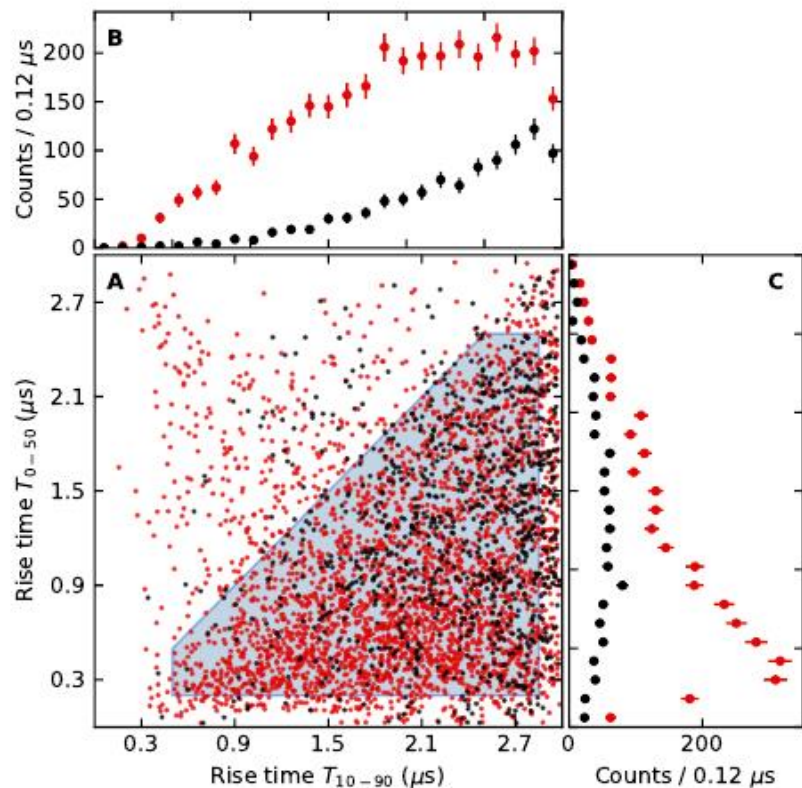


Figure 7.10: A: Two dimensional rise-time distributions for events in the ^{133}Ba calibration data set that pass all quality cuts with an additional Cherenkov cut of $N_{\text{iw}}^{\text{min}} = 5$. Only events with an energy of $5 \leq N_{\text{pe}} \leq 20$ are shown. Red (black) data points represent the \mathcal{C} (\mathcal{AC}) data set. The shaded blue region represents one of the proposed rise-time cuts. B: T_{10-90} distribution marginalized over T_{0-50} . C: T_{0-50} marginalized over T_{10-90} . An excess of coincidence events over anti-coincidences is readily visible in all panels.

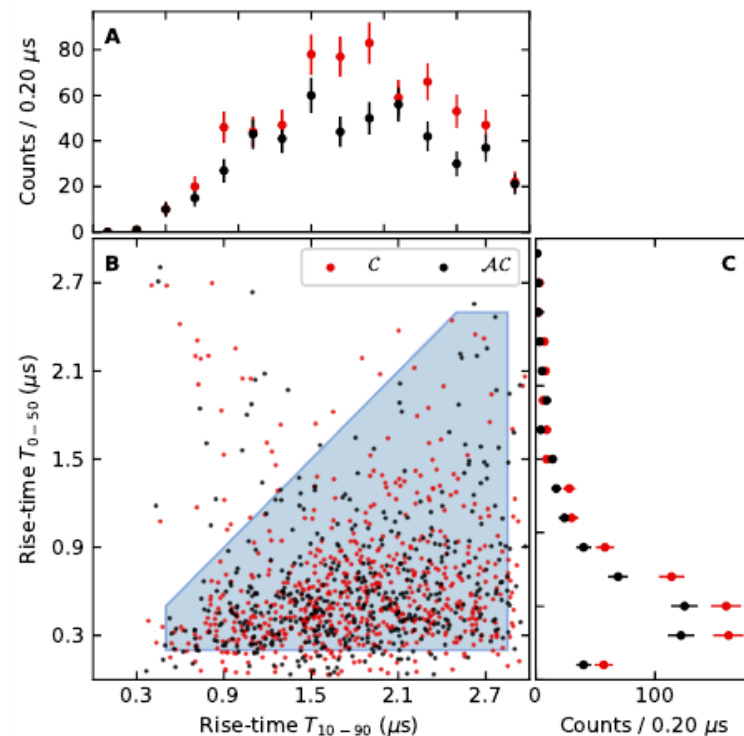


Figure 9.19: Rise-time distributions of \mathcal{ON} events passing all optimized data cuts during $\text{CE}\nu\text{NS}$ search runs. The \mathcal{C} (\mathcal{AC}) data is shown in red (black). The events of both data sets mainly cluster around the same rise-times seen in Fig. 7.11. In addition an excess is readily visible for the \mathcal{C} data over the \mathcal{AC} data, which is caused by $\text{CE}\nu\text{NS}$ -induced events. This excess is therefore fully comprised of nuclear recoils. The residual $\mathcal{R} = \mathcal{C} - \mathcal{AC}$ is shown in Fig. 9.20. A tail above the $T_{0-50} = T_{10-90}$ diagonal can be identified, that is caused by misidentified event onsets due to a preceding SPE. The shaded blue region shows the optimized rise-time cut window.

